Electronic Supplementary Material (ESI) for Journal of Materials Chemistry A.

Supplementary Information

Generalizable, Tunable Control of Divalent Cation Solvation Structure via Mixed Anion Contact Ion Pair Formation

Sydney N. Lavan[1,2], *Stefan Illic*[1,2], *Shashwat Viswanath*[1,2], *Akash Jain*[1,2], *Rajeev S. Assary*[1,2] *and Justin G. Connell*[1,2*]

[1] *Joint Center for Energy Storage Research, Argonne National Laboratory, Lemont, IL 60439, USA*

[2] *Materials Science Division, Argonne National Laboratory, Lemont, IL 60439, USA*

** Email: jconnell@anl.gov*

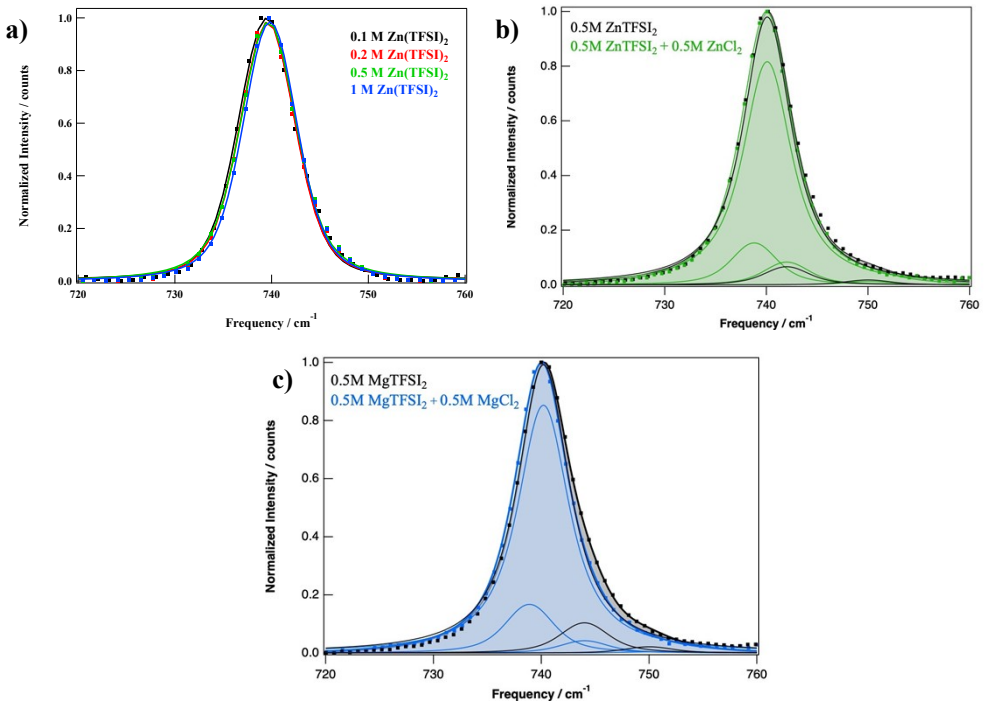

Figure S1. (a) $ZnTFSI_2$ concentration dependence Raman spectra of the $TFSI^-$ breathing mode. (b) Higher concentration of 1M $ZnTFSI_2$ in black compared to 1:1 ratio of $ZnTFSI_2$:$ZnCl_2$ in green. (c) Higher concentration of 1M $MgTFSI_2$ in black compared to 1:1 ratio of $MgTFSI_2$:$MgCl_2$ in blue.

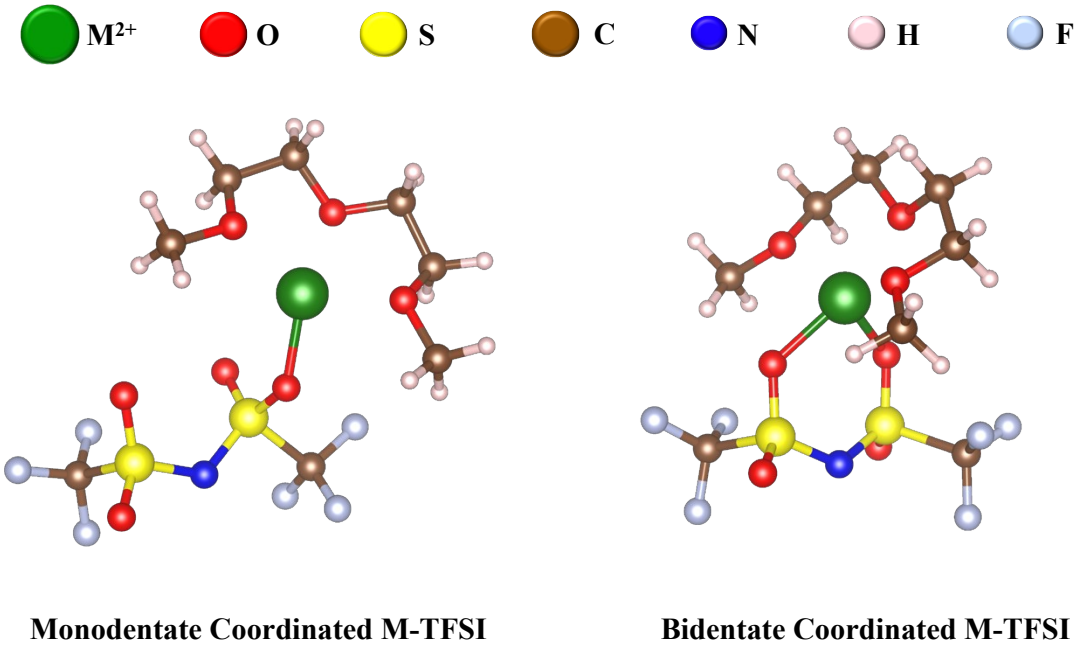

Figure S2. DFT modeled structures of metal cation (M=Zn, Mg and Cu) coordinated to TFSI in a mono- or bidentate configuration with an explicit G2 molecule. $M(TFSI)^{mono}(G2)$ and $M(TFSI)^{bi}(G2)$

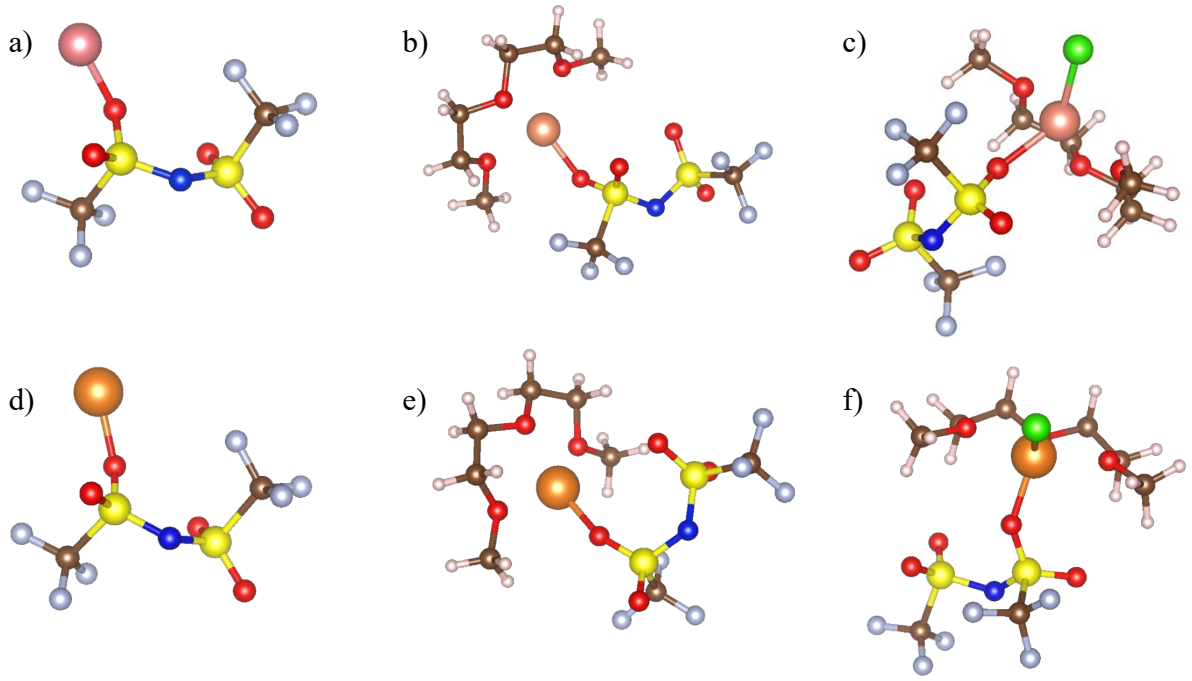

Figure S3. Optimized morphologies of the 6 DFT structures studied. Zn is top row a-c and Mg is bottom row d-f.

Table S1. DFT computed free energy of the six (1 to 6) complexation reactions.

Reactants	Products	Calculated ΔG
1. Mg + 2G2 + TFSI	**Mg-TFSI + 2G2**	**-0.09 eV**
2. 2 Mg + 2G2 + 2Cl + 2TFSI	**2Mg-TFSI-Cl + 2G2**	**-1.28 eV**
3. Zn + 2G2 +TFSI	**Zn-TFSI + 2G2**	**-0.04 eV**
4. 2 Zn + 2G2 +2Cl + 2TFSI	**2Zn-TFSI-Cl + 2G2**	**-1.61 eV**
5. Cu + 2G2 + TFSI	**Cu-TFSI^{+} + 2G2**	**-0.18 eV**
6. 2Cu + 2G2 + 2Cl + 2TFSI	**2Cu-TFSI-Cl +2G2**	**-1.75 eV**

For the calculated free energies, we divided the overall value by two for reactions 2, 4 and 6 to enable direct comparison with the energies calculated in reactions 1, 3 and 5.

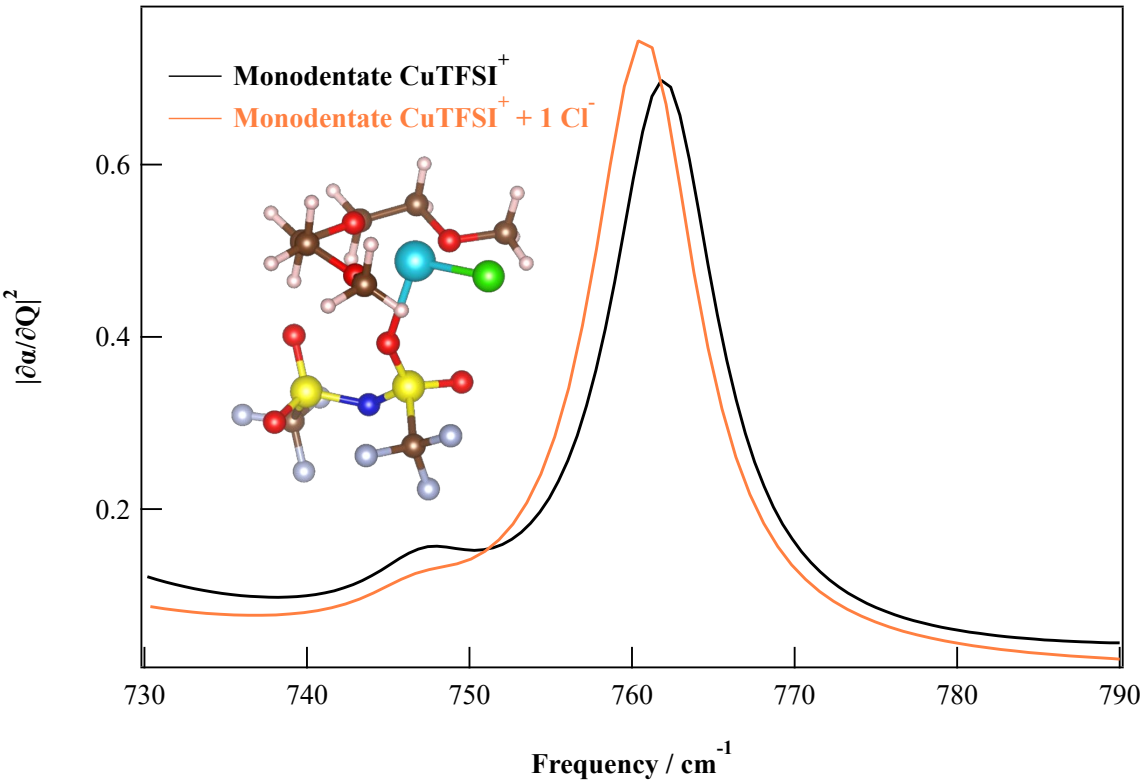

Figure S4. DFT calculated Raman spectra for Cu(TFSI)^{mono}(G2) and Cu(TFSI)^{mono}(Cl)(G2).

Table S2. Relative percent populations of the different TFSI$^-$/halide ratios solvation environments for zinc determined from fitting of experimental Raman data.

Solvation Structure	0.1M $ZnTFSI_2$	0.1M $ZnTFSI_2$ + 0.025M $ZnCl_2$	0.1M $ZnTFSI_2$ + 0.05M $ZnCl_2$	0.1M $ZnTFSI_2$ + 0.1M $ZnCl_2$	0.1M $ZnTFSI_2$ + 0.2M $ZnCl_2$
Zn(TFSI)^{mono}(Cl)	-	13%	16%	40%	41%
"Free" TFSI$^-$	95%	82%	79%	54%	56%
Zn(TFSI)^{mono}	2%	3%	3%	3%	3%
Zn(TFSI)^{bi}	3%	2%	2%	3%	-

Table S3. Relative percent populations of the different TFSI$^-$/halide ratios solvation environments for magnesium determined from fitting of experimental Raman data.

Solvation Structure	0.1M $MgTFSI_2$	0.1M $MgTFSI_2$ + 0.025M $MgCl_2$	0.1M $MgTFSI_2$ + 0.05M $MgCl_2$	0.1M $MgTFSI_2$ + 0.1M $MgCl_2$	0.1M $MgTFSI_2$ + 0.2M $MgCl_2$
Mg(TFSI)^{mono}(Cl)	-	20%	43%	51%	61%
"Free" TFSI$^-$	89%	71%	49%	43%	36%
Mg(TFSI)^{mono}	9%	7%	6%	3%	1%
Mg(TFSI)^{bi}	2%	2%	2%	2%	2%

Table S4. Relative percent populations of the different $TFSI^-$/halide ratios solvation environments for calcium determined from fitting of experimental Raman data.

Solvation Structure	0.1M $CaTFSI_2$	0.1M $CaTFSI_2$ + 0.025M $CaCl_2$	0.1M $CaTFSI_2$ + 0.05M $CaCl_2$	0.1M $CaTFSI_2$ + 0.1M $CaCl_2$	0.1M $CaTFSI_2$ + 0.2M $CaCl_2$
$Ca(TFSI)^{mono}(Cl)$	-	38%	36%	19%	19%
"Free" $TFSI^-$	48%	33%	36%	56%	56%
$Ca(TFSI)^{mono}$	4%	7%	6%	2%	4%
$Ca(TFSI)^{CIP}$	31%	13%	15%	14%	13%
$Ca(TFSI)^{bi}$	17%	8%	8%	9%	8%

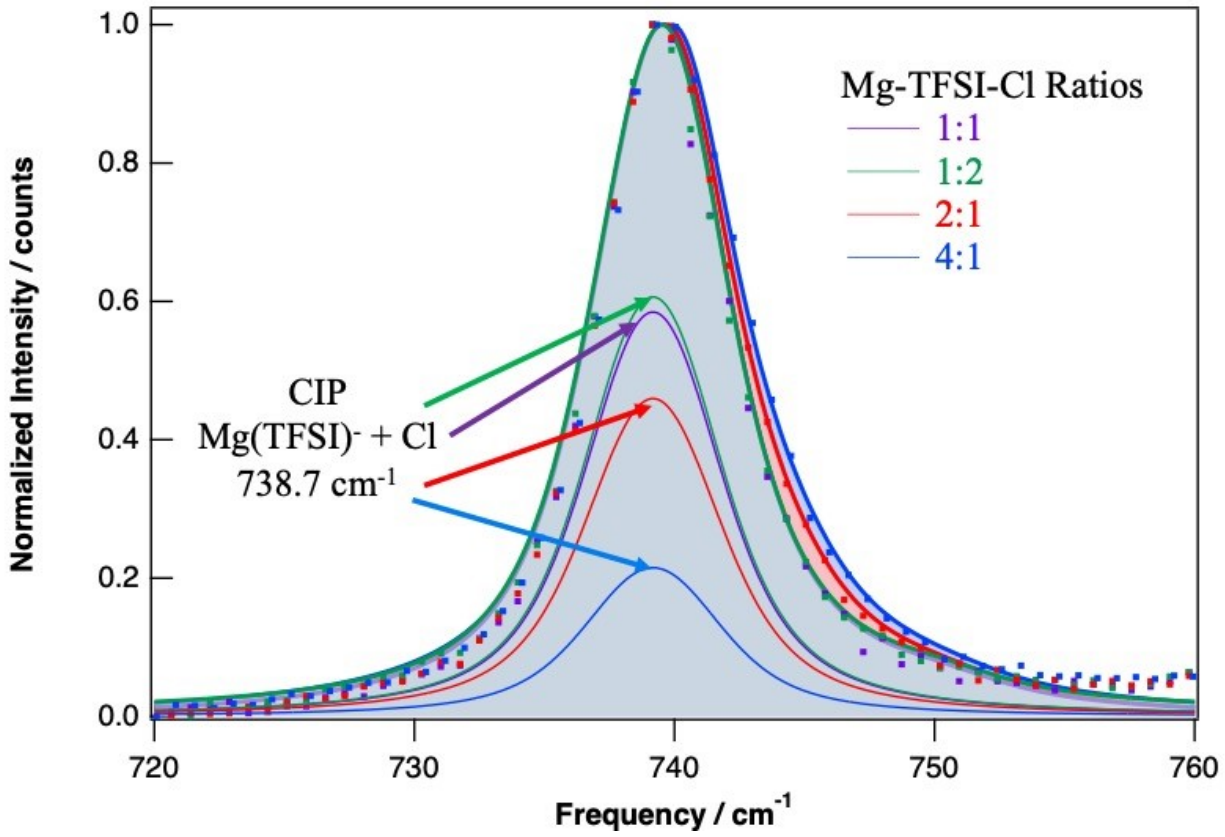

Figure S5. Experimental Raman spectra of Mg-TFSI:Cl ratio. Highlighting the evolution of the mixed contact ion pair.